
Optimized Deformed Laplacian for Spectrum-based Community Detection in Sparse Heterogeneous Graphs

Lorenzo Dall’Amico¹ Romain Couillet^{1,2} Nicolas Tremblay¹

Abstract

Spectral clustering is one of the most popular, yet still incompletely understood, methods for community detection on graphs. In this article we study spectral clustering based on the deformed Laplacian matrix $D - rA$, for sparse heterogeneous graphs (following a two-class degree-corrected stochastic block model). For a specific value $r = \zeta$, we show that, unlike competing methods such as the Bethe Hessian or non-backtracking operator approaches, clustering is insensitive to the graph heterogeneity. Based on heuristic arguments, we study the behavior of the informative eigenvector of $D - \zeta A$ and, as a result, we accurately predict the clustering accuracy. Via extensive simulations and application to real networks, the resulting clustering algorithm is validated and observed to systematically outperform state-of-the-art competing methods.

1. Introduction

Graphs are ubiquitous mathematical objects to represent networks of items and their connections. One of the most natural unsupervised machine learning tasks consists in recognizing structures inside a graph \mathcal{G} and clustering its n nodes in a partition of groups sharing similar properties. Such algorithms find important applications in a variety of fields spanning from social sciences to biological and technological networks (Fortunato & Hric, 2016).

The clustering problem is generally very hard to solve and has found rigorous and efficient solutions only in particularly homogeneous regimes. The best performing algorithm so far is belief propagation, as repeatedly confirmed by simulations (see subsequent references), that however is penalized by its high computational cost, its mathematical intractability, and its lack of convergence guarantee for arbitrary initial conditions. Performances close to belief

propagation are much simpler reached via spectral clustering, by exploiting the eigenvectors of properly chosen graph representative matrices (Rohe et al., 2011; Von Luxburg, 2007; Gulikers et al., 2017; Lei & Rinaldo, 2015). Among those matrices, the most commonly chosen are the adjacency matrix¹ A , the Laplacian² $D - A$, the symmetric normalized Laplacian $D^{-\frac{1}{2}}AD^{-\frac{1}{2}}$ and the random walk Laplacian $D^{-1}A$. All these matrices exploit the fact that nodes belonging to the same affinity “class” are more likely to get connected to one another. It is worth pointing out for further reference that the early arguments brought forth to propose these algorithms usually assumed rather dense and easily classifiable graph settings (Von Luxburg, 2007). In addition to performing well and being computationally attractive, spectral methods are also mathematically easy to manipulate, particularly in the dense regime where the average node degree scales like the size of the network. In this regime, random matrix theory (Nadakuditi & Newman, 2012; Tiomoko Ali & Couillet, 2016) manages to predict the asymptotic clustering performances and to identify transition points beyond which asymptotic non trivial classification is achievable.

Real networks however tend not to be dense, as the average degree usually does not scale with n . For these *sparse* networks, the aforementioned spectral methods no longer bring competitive performance with respect to belief propagation. Besides, random matrix theory is in general unable to provide accurate insights on the sparse graph problem. Many intuitions have instead emerged from statistical physics which have led important seminal steps in understanding the clustering problem in sparse networks. Notably, two deeply connected matrices have recently proved to overcome the problem of sparsity: the Bethe Hessian (Saade et al., 2014)

$$H_r = (r^2 - 1)I_n + D - rA \quad (1)$$

for some well-chosen $r \in \mathbb{R}$, and the (non symmetric) non backtracking operator $B \in \mathbb{R}^{2m \times 2m}$ (with $m = |\mathcal{E}|$ the

¹Univ. Grenoble Alpes, CNRS, Grenoble INP, GIPSA-lab, Grenoble, France ²L2S, CentraleSupélec, University of Paris Saclay, France. Correspondence to: Lorenzo Dall’Amico <lorenzo.dall-amico@gipsa-lab.grenoble-inp.fr>.

¹The adjacency matrix is defined as $A_{ij} = \mathbb{1}[(ij) \in \mathcal{E}]$, where \mathcal{E} is the set of edges of the graph $\mathcal{G} = \mathcal{G}(\mathcal{E}, \mathcal{V})$ and \mathcal{V} the set of nodes ($\mathbb{1}[\cdot]$ is the indicator function).

²The matrix D is the diagonal degree matrix defined as $D_{ij} = \delta_{ij} \sum_j A_{ij}$, where δ_{ij} is the Kronecker symbol.

number of edges) (Krzakala et al., 2013) with

$$B_{(ij)(kl)} = \delta_{jk}(1 - \delta_{il}) \quad (2)$$

for all $i, j, k, l \in \mathcal{V}$ such that $A_{ij}A_{kl} = 1$. In a two-class setting (as assumptions go so far), the informative eigenvector of H_r is the one associated with the second smallest eigenvalue, and for B the one attached to the eigenvalue with second largest amplitude (which happens to be real). An important link, that we shall later exploit, relates the matrices B and H_r (Terras, 2010; Bordenave et al., 2015):

$$\exists u \neq 0, Bu = \gamma u \Leftrightarrow \det[H_\gamma] = 0. \quad (3)$$

Most of the motivation and intuitions of the aforementioned methods stem from the analysis of large random networks generated according to a two-class stochastic block model (SBM). Denoting $\sigma \in \{-1, 1\}^n$ the vector of class labels, the SBM generates edges with probability $\mathbb{P}(A_{ij} = 1 | \sigma_i, \sigma_j) = C(\sigma_i, \sigma_j)$ where $C(\sigma_i, \sigma_j) = c_{\text{in}}/n$ if $\sigma_i = \sigma_j$ and $C(\sigma_i, \sigma_j) = c_{\text{out}}/n$ otherwise. The factor $1/n$ in the probability makes the average degree independent of the network size and hence sparse by definition.

The above matrices B and H_r for $r = \sqrt{\rho(B)}$ – with $\rho(\cdot)$ the spectral radius – have proved to perform better than conventional spectral methods for sparse two-class SBM graphs with equal size classes. Importantly, they perform non trivially down to the optimal detectability threshold, that is whenever

$$\alpha \equiv \frac{c_{\text{in}} - c_{\text{out}}}{\sqrt{c}} > 2, \text{ where } c \equiv \frac{c_{\text{in}} + c_{\text{out}}}{2}.$$

This inequality has been proved optimal in the sense that community detection is asymptotically impossible if the condition is not met (Massoulié, 2014; Mossel et al., 2015).

The SBM model is however often considered too simple to account for the degree heterogeneity of real graphs. In the present article, we thus rather focus on the problem of clustering on a graph generated from a degree corrected stochastic block model (DC-SBM), *i.e.*, with

$$\mathbb{P}(A_{ij} = 1 | \sigma_i, \sigma_j, q_i, q_j) = q_i q_j C(\sigma_i, \sigma_j) \quad (4)$$

where $\mathbf{q} = (q_i)_{i=1}^n \in \mathbb{R}^n$ is the vector of random i.i.d. intrinsic connection probabilities, independent of the classes, and such that $\mathbb{E}[q_i] = 1$. Important results on spectral clustering were obtained for this model either in the dense regime with appropriate adaptations of the Laplacian matrix (Tiomoko Ali & Couillet, 2016) and in the sparse case for the non backtracking operator (Gulikers et al., 2015; 2016). In the latter work it was shown that in the DC-SBM setting the detectability threshold is updated as

$$\alpha \equiv \frac{c_{\text{in}} - c_{\text{out}}}{\sqrt{c}} > \alpha_c \equiv \frac{2}{\sqrt{\Phi}}, \quad \Phi \equiv \mathbb{E}[q_i^2]. \quad (5)$$

Also it was proved that, when the inequality is met, B has exactly two real eigenvalues outside its main bulk and that the eigenvector related to the second largest is correlated to the class labels σ . Performing spectral decomposition on B is however computationally expensive, scaling in size with the number of edges rather than the number of nodes.

In the present work we propose a spectral method with an $n \times n$ matrix akin to the Bethe Hessian operator, able to perform clustering on a sparse graph generated with the DC-SBM model. The object of our study is the deformed Laplacian (Grindrod et al., 2018; Morbidi, 2013) (or r-Laplacian (Banks et al., 2014)) matrix

$$D - rA$$

however taken for a fundamentally different value of r than proposed in (Saade et al., 2014) for the SBM model. We precisely realize that:

- for a specific choice $r = \zeta$, on average, spectral clustering on $D - \zeta A$ is effective and, most importantly, does not suffer the heterogeneity of the degrees (unlike $H_{\sqrt{\rho(B)}}$ proposed in (Saade et al., 2014));
- through extensive simulations on both synthetic and real graphs, we show that this method systematically outperforms or at least equals competing ones;
- this matrix is not arbitrary: we draw important connections between $D - \zeta A$ and (a) the non-backtracking matrix B since ζ can be mapped to an isolated eigenvalue *inside* the main “bulk” of the spectrum of B , visible in all articles but never raised by the authors, (b) the popular “random walk” Laplacian $D^{-1}A$ that we claim has an informative eigenvector that behaves essentially like that of $D - \zeta A$ *but* the latter is associated with an eigenvalue possibly deep in the bulk: this is a new observation that explains the observed limitations of $D^{-1}A$ in the sparse regime but at the same time “rehabilitates” spectral clustering on $D^{-1}A$ (provided the informative eigenvector is identified).

The remainder of the article is organized as follows: Section 2 formally introduces the problem and notations and gives an argument for the choice of ζ ; based on heuristic rather than purely theoretical arguments, Section 3 studies the behavior of the informative eigenvector and its associated “noise”, concluding with an explicit expression of the expected performance of the algorithm closely matching experimental results; Section 4 draws connections with the aforementioned competing methods; numerical supports are then provided in Section 5, also testing our proposed algorithm on commonly used real networks; concluding remarks close the article in Section 6.

Reproducibility. A Python implementation of the proposed algorithm along with codes to reproduce the

results of the article are available for download at <https://lorenzodallamico.github.io/codes/>.

2. Model and Preliminaries

Consider an undirected binary graph $\mathcal{G}(\mathcal{E}, \mathcal{V})$, where $\mathcal{V} = \{1, \dots, n\}$ is the set of nodes ($|\mathcal{V}| = n$) and $\mathcal{E} \subset \mathcal{V} \times \mathcal{V}$ ($|\mathcal{E}| = m$) the set of edges. Let $\boldsymbol{\sigma} \in \{-1, 1\}^n$ be a vector that attributes (class) labels to each node, and assume the two classes of even size. We consider the earlier defined degree corrected stochastic block model (DC-SBM) as a generative model (*i.e.*, from (4)) for \mathcal{G} .

The core of our proposed method lies in a very elementary observation, related to the action of $D - rA$ on vector $\boldsymbol{\sigma}$:

$$[(D - rA)\boldsymbol{\sigma}]_i = d_i \sigma_i \left[1 - r \left(\frac{|\partial_i^{(s)}|}{d_i} - \frac{|\partial_i^{(o)}|}{d_i} \right) \right] \quad (6)$$

where $|\partial_i^{s/o}|$ stands for the number of neighbors of i belonging to the same (s) and to the opposite (o) class as i .

We intend to show that a proper choice of r can annihilate the right-hand side of (6) “on average” or whenever the typical degrees d_i are not too small. This turns (6) into an eigenvector equation. To this end, we need to quantify the random variables $|\partial_i^{(s)}|$ and $|\partial_i^{(o)}|$. Taking a Bayesian inference perspective, we may see $\boldsymbol{\sigma}$ and \boldsymbol{q} as unknown parameters and A (and d_i) as known realizations, and have:

$$\begin{aligned} \mathbb{P}(\sigma_i, \sigma_j | A_{ij} = 1) &= \iint \mathbb{P}(\sigma_i, \sigma_j, q_i, q_j | A_{ij} = 1) dq_i dq_j \\ &\propto \iint \mathbb{P}(A_{ij} = 1 | \sigma_i, \sigma_j, q_i, q_j) \mathbb{P}(\sigma_i, \sigma_j, q_i, q_j) dq_i dq_j \\ &\propto C(\sigma_i, \sigma_j) \iint q_i q_j \mathbb{P}(q_i) \mathbb{P}(q_j) dq_i dq_j = C(\sigma_i, \sigma_j) \end{aligned}$$

where we used the facts that the blocks are of equal size ($\mathbb{P}(\sigma_i)$ is constant), and that the q_i are i.i.d., independent of the classes and of expected value 1. Normalizing, one finally obtains $\mathbb{P}(\sigma_i, \sigma_j | A_{ij} = 1) = nC(\sigma_i, \sigma_j)/[2(c_{\text{in}} + c_{\text{out}})]$ and thus $\mathbb{P}(\sigma_i = \sigma_j | A_{ij} = 1) = c_{\text{in}}/(c_{\text{in}} + c_{\text{out}})$. We further know that $|\partial_i^{(s)}| + |\partial_i^{(o)}| = d_i$ which is a deterministic observation. We hence see $|\partial_i^{(s)}|$ as the sum of d_i i.i.d. Bernoulli random variables with parameter $p = c_{\text{in}}/(c_{\text{in}} + c_{\text{out}})$, so that

$$\begin{aligned} \mathbb{E}(|\partial_i^{(s)}| | A) &= d_i c_{\text{in}} / (c_{\text{in}} + c_{\text{out}}) \\ \mathbb{E}(|\partial_i^{(o)}| | A) &= d_i c_{\text{out}} / (c_{\text{in}} + c_{\text{out}}) \end{aligned}$$

from which we thus obtain

$$\mathbb{E}([(D - rA)\boldsymbol{\sigma}]_i | A) = d_i \sigma_i \left(1 - r \frac{c_{\text{in}} - c_{\text{out}}}{c_{\text{in}} + c_{\text{out}}} \right).$$

This equation suggests that, for (6) to be an approximate eigenvector equation in the large- d_i regime, r should be taken equal to

$$\zeta \equiv \frac{c_{\text{in}} + c_{\text{out}}}{c_{\text{in}} - c_{\text{out}}} \equiv \zeta_\alpha = \frac{2\sqrt{c}}{\alpha}. \quad (7)$$

with α as in (5) the proper control parameter for the clustering problem (as shown *e.g.*, in (Nadakuditi & Newman, 2012; Decelle et al., 2011; Gulikers et al., 2015; 2016)). For simplicity of notation the dependence on α of ζ will be made explicit only when relevant.

In practice, c_{in} and c_{out} are however unknown and thus ζ is not directly accessible. Estimates for ζ are later provided.

Remark 1 (Consistency of ζ for trivial classification). *For trivial clustering (as $c_{\text{out}} \rightarrow 0$), $|\partial_i^{(s)}|$ and $|\partial_i^{(o)}|$ exactly tend to their mean. In particular, for $c_{\text{out}} = 0$, $\zeta = 1$ and $(D - \zeta A)\boldsymbol{\sigma} = (D - A)\boldsymbol{\sigma} = 0$, so that $\boldsymbol{\sigma}$ is an exact eigenvector of $D - \zeta A$ associated with its zero eigenvalue.*

In practice, for finite d_i and non-trivial classification, zero is not an exact eigenvalue of $D - \zeta A$ and $\boldsymbol{\sigma}$ not an exact eigenvector. By a perturbation analysis around $\boldsymbol{\sigma}$, we next analyze the behavior of the corresponding eigenvector of $D - \zeta A$ and theoretically predict the overlap performance.

3. Insights and Performance Analysis

Given the sparse graph setting under study, standard tools from random matrix theory are ineffective as they do not allow for a simple spectrum analysis of $D - \zeta A$. We here instead provide an intuitive line of arguments on the scaling of various parameters at play using an *expansion on large average degree*. That is, we shall assume a setting where the average degree $c = (c_{\text{in}} + c_{\text{out}})/2$ is such that

$$n \gg c \gg 1.$$

3.1. General behavior of the eigenvector

We start by considering the following exact eigenvalue equation, for $\boldsymbol{\delta} \in \mathbb{R}^n$, $\lambda_\alpha \in \mathbb{R}$ and arbitrary $c_{\text{in}}, c_{\text{out}}$

$$(D - \zeta_\alpha A)(\boldsymbol{\sigma} + \boldsymbol{\delta}) = \lambda_\alpha(\boldsymbol{\sigma} + \boldsymbol{\delta}). \quad (8)$$

Writing $|\partial_i^s| = \mathbb{E}[|\partial_i^s|] + \Delta_i$ and $|\partial_i^o| = \mathbb{E}[|\partial_i^o|] - \Delta_i$,³ where we exploited the relation $|\partial_i^s| + |\partial_i^o| = d_i$, we obtain:

$$[(D - \zeta_\alpha A)(\boldsymbol{\sigma} + \boldsymbol{\delta})]_i = -2\zeta_\alpha \sigma_i \Delta_i + d_i \delta_i - \zeta_\alpha \sum_{k \in \mathcal{N}(i)} \delta_k \quad (9)$$

with $\mathcal{N}(i) \subset \mathcal{V}$ standing for the neighbors of node i (*i.e.*, the j 's such that $A_{ij} = 1$). The random variable Δ_i is a sum

³ Here \mathbb{E} is understood with respect to $\boldsymbol{\sigma}$ only, given A .

of d_i independent (centered) Bernoulli random variables, tending in the large c limit to a zero mean Gaussian,

$$\Delta_i \simeq \mathcal{N}(0, d_i c_{\text{in}} c_{\text{out}} / (c_{\text{in}} + c_{\text{out}})^2) \equiv \mathcal{N}(0, d_i f_\alpha^2 / c_\alpha^2)$$

where we introduced

$$f_\alpha \equiv \frac{\sqrt{c_{\text{in}} c_{\text{out}}}}{c_{\text{in}} - c_{\text{out}}} = \frac{1}{\alpha} \sqrt{c - \frac{\alpha^2}{4}}. \quad (10)$$

Our analysis of (9) relies on the following claim (referred to here as an assumption for mathematical analysis), that we shall justify next.

Assumption 1. *The random variables δ_i , $1 \leq i \leq n$, are distributed as*

$$\delta_i \sim \mathcal{N}(-\mu_\alpha \sigma_i, f_\alpha^2 \beta_i^2)$$

for some $\mu_\alpha \in \mathbb{R}$ depending on α only, and $\beta_i \in \mathbb{R}$ depending on i . Besides, the δ_i 's are "weakly dependent" in the sense that $\mathbb{E}[\delta_i \delta_j] = \mathbb{E}[\delta_i] \mathbb{E}[\delta_j] + O(1/c)$.

We now discuss the details of Assumption 1:

- *Weak dependence:* this claim follows from the weak dependence of the Δ_i 's, which results from the sparse (and thus locally tree-like) nature of the graph.
- *Gaussianity:* Equation (9) features three random variables, the leftmost being Gaussian and the rightmost being the sum of d_i random variables tending to an (asymptotically independent) Gaussian. It is thus reasonable that δ_i be Gaussian so to ensure (8), yet not independent of Δ_i and $\sum_{k \in \mathcal{N}(i)} \delta_k$.
- *Mean of δ_i :* The symmetry of the problem at hand (equal class sizes, same affinity c_{in} for each class), along with the fact that the right-hand side of (6) vanishes in its first order approximation in d_i (or c), suggest that the mean of δ_i does not depend in the first order on d_i but only on σ_i . The amplitude of the mean then depends on α characterized here through μ_α .
- *Variance of δ_i :* the variance appears as the product of two terms: one that depends on i (β_i) and one that depends on α . This follows from assuming that the fluctuations of δ_i follow the fluctuations of Δ_i for which the variance is similarly factorized.

These four arguments are quite natural and, if any, only the specification for the variance of δ_i is a disputable claim. This intuition is supported by simulations in Section 5.

We now need to identify the terms β_i and μ_α introduced in Assumption 1 to track the behavior of δ and thus of the eigenvector $\sigma + \delta$. A first constraint on δ follows from imposing the normalization of the eigenvector which, in the trivial limit equals σ , the norm of which is \sqrt{n} . As such,

$$\|(1 - \mu_\alpha)\sigma + f_\alpha \beta \odot \mathbf{N}\|^2 = n \quad (11)$$

where $\beta = (\beta_i)_{i=1}^n$, and \mathbf{N} is a vector of zero mean and unit variance Gaussian random variables. Denoting $n\tilde{\beta}^2 \equiv \|\beta \odot \mathbf{N}\|^2$ and observing that $\tilde{\beta} = O(\beta_i)$, we can rewrite this equation under the form:

$$(1 - \mu_\alpha)^2 + f_\alpha^2 \tilde{\beta}^2 = 1. \quad (12)$$

This provides a first relation between μ_α and $\tilde{\beta}$. To obtain our next equations, we now explore boundary conditions on the model parameters in the limit of trivial clustering and at the phase transition where clustering becomes impossible.

3.2. Boundary conditions

It is established in (Gulikers et al., 2015) that there exists a critical value $\alpha_c \equiv 2/\sqrt{c\Phi}$ for α below which community detection is (asymptotically) impossible. In particular, for $\alpha = \alpha_c$, the eigenvector $\sigma + \delta$ does not contain any information about the classes and thus $\mu_{\alpha_c} = 1$. From Equation (10), we then find that

$$f_{\alpha_c} = \frac{1}{\alpha_c} \sqrt{c - \frac{\alpha_c^2}{4}} = \frac{1}{2} \sqrt{c\Phi - 1}.$$

Also, from (12), we get $\tilde{\beta} = 1/f_{\alpha_c}$. Updating (12), we now have an explicit expression for μ_α for all α . Recalling that $4f_\alpha^2 = \zeta_\alpha^2 - 1$ (from (7) and (10)) then gives

$$1 - \mu_\alpha = \sqrt{\frac{c\Phi - \zeta_\alpha^2}{c\Phi - 1}}. \quad (13)$$

Getting back to (8) and (9), it now remains to estimate β_i , which we shall perform in the limit $\alpha \rightarrow \sqrt{2c_{\text{in}}}$ of trivial clustering. To this end, combining both equations, we have

$$\begin{aligned} 2f_\alpha(1 - \mu_\alpha)\sqrt{d_i}\tilde{N}_i - \zeta_\alpha \sum_{k \in \mathcal{N}(i)} f_\alpha \beta_k N_k + d_i f_\alpha \beta_i N_i \\ = \lambda_\alpha [(1 - \mu_\alpha)\sigma_i + f_\alpha \beta_i N_i] \end{aligned}$$

for $\tilde{N}_1, N_1, \dots, \tilde{N}_n, N_n$ all (non independent) standard normal random variables. The second left-hand side term is proportional to $\sqrt{d_i}$ (and thus of order $O(\sqrt{c})$) as per the weak independence assumption of the N_k 's (Assumption 1). Dividing both sides by $f_\alpha \sqrt{d_i}$ to equate terms of order $O(1)$, the right-hand side now scales as $\lambda_\alpha / (f_\alpha \sqrt{d_i})$. As noted in Remark 1, in the trivial clustering limit where $\alpha \rightarrow \sqrt{2c_{\text{in}}}$, $\lambda_\alpha \rightarrow 0$, but it is not clear whether the right-hand side (after division by $f_\alpha \sqrt{d_i}$) vanishes; we now investigate this term in detail. One may at first observe that, if $c_{\text{out}} = \epsilon c_{\text{in}}$ for $\epsilon \ll 1$, since c typically scales like d_i , we obtain that $f_\alpha \sqrt{d_i} = \sqrt{\epsilon c_{\text{in}}/2} + O(\epsilon)$. Hence, if $c_{\text{in}} \gtrsim \epsilon^{-1}$, the right-hand side vanishes. But imposing this growth condition is in fact not even necessary. If $\lambda_\alpha \propto f_\alpha^\tau$ for some $\tau > 1$, we directly obtain a vanishing right-hand side term; we will comment later that $\tau = 2$ (see (16)).

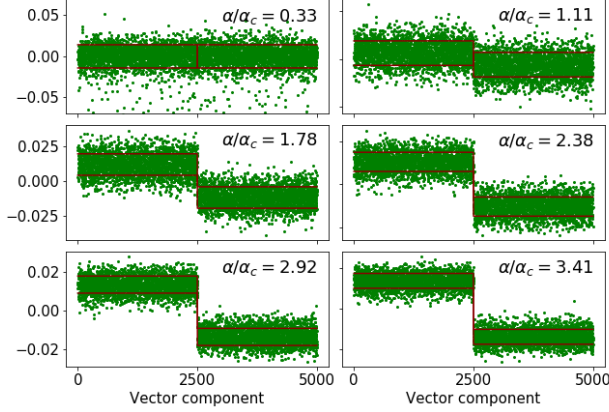


Figure 1. Comparison of the theoretical values of mean and variance (the red line indicates $1 - \mu_\alpha \pm f_\alpha \tilde{\beta}$) with the simulations results (green dots) for Cauchy distributed q_i 's. The following parameters were used: $n = 5000$, $c_{\text{out}} = 20$, $c_{\text{in}} = 23 \rightarrow 81$.

Denoting $\sum_{k \in \mathcal{N}(i)} \beta_k N_k \equiv \langle \beta \rangle N \sqrt{d_i}$ for some $\langle \beta \rangle > 0$, we may then rewrite

$$2(1 - \mu_\alpha) \tilde{N}_i - \zeta_\alpha \langle \beta \rangle N + \sqrt{d_i} \beta_i N_i \rightarrow 0 \quad (14)$$

in the limit $\alpha \rightarrow \sqrt{2c_{\text{in}}}$. Besides, $\mu_\alpha \rightarrow 0$ while $\zeta_\alpha \rightarrow 1$. We already argued that β_i (and thus $\langle \beta \rangle$), which is of the order of $\tilde{\beta}$, scales as $1/f_{\alpha_c} = O(c^{-1/2})$. Thus, in the limit of large degrees, the second term in (14) is negligible and the third of order $O(1)$. Equating the large degree limiting variances of the resulting equation finally gives

$$\beta_i = \frac{2}{\sqrt{d_i}}.$$

3.3. Estimating the overlap

The previous line of arguments provides us with “first-order” approximations (with respect to c) for all relevant quantities involved in the study of $\sigma + \delta$. This in turn yields an approximation for the performance of spectral clustering based on this eigenvector. The performance measure of interest is the *overlap*

$$\text{Ov} \equiv 2 \left[\frac{1}{n} \sum_{i=1}^n \delta_{\sigma_i, \hat{\sigma}_i} - \frac{1}{2} \right]$$

where $\hat{\sigma}$ is the vector of the estimated σ , and $\delta_{\sigma_i, \hat{\sigma}_i} = 1$ if $\text{sgn}((\sigma_i + \delta_i)\sigma_i) > 0$ and 0 otherwise. Considering a node with $\sigma_i = 1$ without loss of generality, in the large c limit,

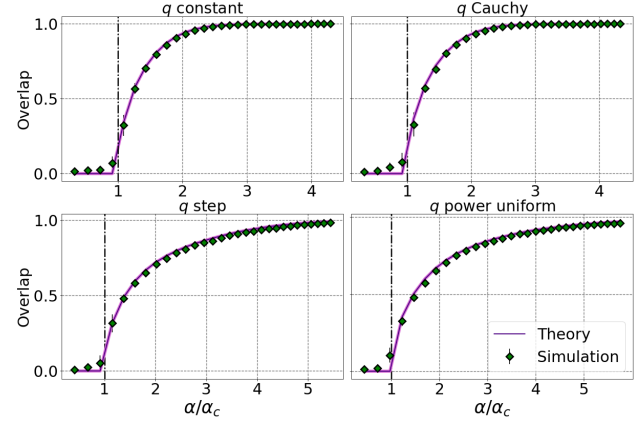


Figure 2. Simulated versus theoretical (15) overlap for q_i distributed as “Constant” (top left), “Cauchy” (top right), “Step” (bottom left) or “Power uniform” (bottom right). $n = 5000$, $c_{\text{out}} = 20$ and $c_{\text{in}} = 23 \rightarrow 81$. Average over 10 realizations.

we have the approximate classification error for node i

$$\begin{aligned} \mathbb{P}_{\text{err}}^i &\simeq \frac{1}{\sqrt{2\pi[f_\alpha \beta_i]^2}} \int_{(1-\mu_\alpha)}^{\infty} e^{-x^2/(2[f_\alpha \beta_i]^2)} dx \\ &= \frac{1}{2} \left[1 - \text{erf} \left(\frac{1}{\sqrt{2}[f_\alpha \beta_i]} (1 - \mu_\alpha) \right) \right]. \end{aligned}$$

We hence obtain the following final explicit expression of the expected overlap, conditionally to A ,

$$\mathbb{E}[\text{Ov}] \simeq \frac{1}{n} \sum_{i=1}^n \text{erf} \left[\sqrt{\frac{\alpha^2 d_i}{8c - 2\alpha^2}} \left(\frac{c\Phi - \zeta_\alpha^2}{c\Phi - 1} \right) \right]. \quad (15)$$

To validate our derivations, we subsequently compare our theoretical results to simulations for q_i stemming from one of the following four distributions subject to $\mathbb{E}[q_i] = 1$:

- **Constant.** $q_i = 1, \forall i \in \mathcal{V}$;
- **Power uniform.** $q_i \sim \frac{1}{Z} U(3, 10)^{3.5}$, with $U(3, 10)$ the uniform distribution over $[3, 10]$;
- **Step.** $q_i \in \{q_{\text{min}}, q_{\text{max}}\}$, with $q_{\text{max}} = 8q_{\text{min}}$;
- **Cauchy.** $q_i \sim \frac{1}{Z} \text{SCauchy}(x_0 = 1.5, \gamma = 0.01)$ where SCauchy is a Cauchy distribution saturated to lower and upper thresholds. See the Python codes for details.

Figure 1 compares the theoretical values of the mean and the variance of each component of the informative eigenvector of $D - \zeta A$ to simulations for a Cauchy distribution of the q_i 's. Figure 2 then displays the theoretical versus numerical overlaps for the four aforementioned distributions of the q_i . Both figures demonstrate a virtually perfect fit between theory and practice, thereby strongly suggesting the validity of our assumption and results.

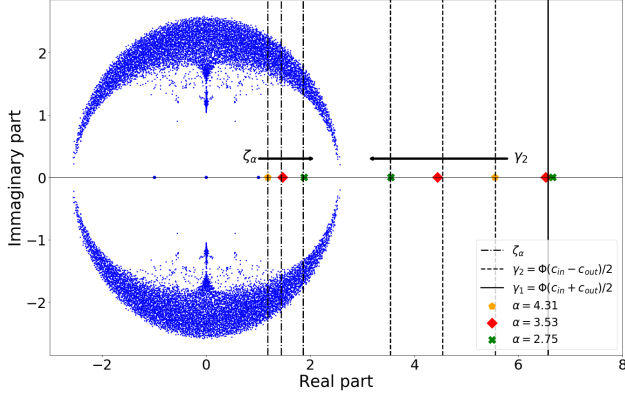


Figure 3. Superposition of the spectra of the matrix B for three different values of α : $n = 3000$, $c_{\text{in}} = [12, 11, 10]$ and $c_{\text{out}} = [1, 2, 3]$ ($c_{\text{in}} + c_{\text{out}}$ is fixed); \mathbf{q} distributed according to SCauchy; all eigenvalues displayed in blue but for top three dominant real eigenvalues displayed in different colors for each pair $(c_{\text{in}}, c_{\text{out}})$.

4. Relation to Alternative Spectral Methods

This section describes how $D - \zeta A$ constitutes an important and natural bridge between statistical physics ideas for community detection on sparse graphs (the Bethe Hessian and the non backtracking matrices) as well as the popular random walk Laplacian operator $D^{-1}A$ approach.

4.1. Connection to the Bethe Hessian

The original intuition of the Bethe Hessian and its name arise from a convenient mapping of the clustering problem to the Ising model on $\mathcal{G}(\mathcal{E}, \mathcal{V})$. Identifying the class labels σ_i as spins, one can express the tendency to connect with nodes of the same class as an energetic gain, in the form of a ferromagnetic interaction with Hamiltonian

$$\mathcal{H}(\sigma) = -J \sum_{(i,j) \in \mathcal{E}} \sigma_i \sigma_j.$$

Letting $r \equiv [\text{th}(\beta J)]^{-1}$, where $\beta = (k_B T)^{-1}$,⁴ the Hessian matrix of the *Bethe free energy at the paramagnetic point* corresponds (up to a constant) to the matrix H_r in (1) (see (Yedidia et al., 2005; Saade et al., 2014) for details).

Authors in (Saade et al., 2014) observe that H_r has two isolated (smallest) eigenvalues $\theta_1(r) < \theta_2(r)$ that separate from the others. They also see from simulations that the eigenvector associated with $\theta_2(r)$ strongly correlates to σ . To determine the optimal r (or optimal temperature T), they note that for large r all eigenvalues of H_r are positive (the system is at the paramagnetic point). As r decreases, $\theta_1(r)$ becomes negative (the system there undergoes ferromagnetic phase transition). The authors next point out that, as r

⁴with k_B the Boltzmann constant and T the temperature.

further decreases, $\theta_2(r)$ also decreases and becomes negative. By further decreasing the temperature to $r = \sqrt{\rho(B)}$ the system undergoes a spin glass phase transition. This is where they claim that r is optimal.

Now, if one continues to reduce the temperature so that $r < \sqrt{\rho(B)}$, $\theta_2(r)$ reverses direction and increases until it crosses zero a second time. This was already observed in (Saade et al., 2014). However, the authors did not realize that, remarkably, according to our extensive simulations, $r \simeq \zeta$ at this second zero-crossing, *i.e.*, we likely have $\theta_2(\zeta) = 0$. Even more strikingly, simulations further suggest that the eigenvector associated with the null eigenvalue of $H_\zeta = (\zeta^2 - 1)I_n + D - \zeta A$ is the informative eigenvector $\sigma + \delta$ studied in Section 3. This indicates that the informative eigenvalue λ_α of $D - \zeta_\alpha A$ in our analysis of Section 3 coincides with $-(\zeta_\alpha^2 - 1)$. This fundamental finding can be summarized as follows.

Claim 1 (Informative Eigenvalue of $D - \zeta_\alpha A$). *The eigenvalue λ_α associated to the informative eigenvector of $D - \zeta_\alpha A$ is given by*

$$\lambda_\alpha = -(\zeta_\alpha^2 - 1) = -4f_\alpha^2 \quad (16)$$

thereby ensuring that the right-hand side of (8) indeed vanishes for $\alpha \rightarrow \sqrt{2c_{\text{in}}}$, as stated in Section 3.

This claim further provides a way to estimate ζ .

Remark 2 (First estimation of ζ). *To estimate ζ one may line-search over $r \in (1, \sqrt{\rho(B)})$ for a change of sign of $\theta_2(r)$, that occurs for $r = \zeta$.⁵*

From (3), this observation has further implications to the spectrum of the non-backtracking operator B which we now discuss (and that also appear to have been missed in the literature).

4.2. Relation to the Non-Backtracking Operator

4.2.1. EXPLOITING EIGENVALUES OUTSIDE THE BULK

The non backtracking matrix $B \in \mathbb{R}^{2m \times 2m}$ defined in (2) was proposed as a potent alternative to the adjacency matrix for community detection in sparse graphs (Krzakala et al., 2013), given its capacity to avoid the spreading of eigenvalues incurred by highly connected nodes (which tend to be numerous in sparse graphs).

It is rigorously proved in (Gulikers et al., 2016) that, for the DC-SBM and beyond the phase transition ($\alpha > \alpha_c$), the eigenvalues $\gamma_1, \dots, \gamma_{2m}$ of B satisfy in the large n setting: $\gamma_1 \rightarrow \Phi(c_{\text{in}} + c_{\text{out}})/2$, $\gamma_2 \rightarrow \Phi(c_{\text{in}} - c_{\text{out}})/2 > \sqrt{\gamma_1}$ and, for $i > 2$, $\limsup_n |\gamma_i| \leq \sqrt{\gamma_1}$. Since $\zeta = \gamma_1/\gamma_2$, this result conveys an alternative estimation method for ζ .

⁵The spectral radius of the matrix B can be estimated as $\rho(B) \simeq \sum_i d_i^2 / \sum_i d_i$.

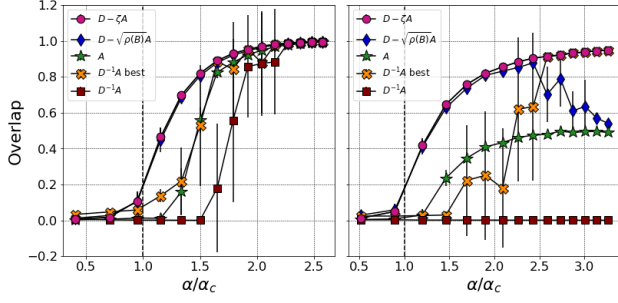


Figure 4. Comparison of spectral clustering methods for q_i following the ‘‘Constant’’ (left) and ‘‘Step’’ (right) distribution. ‘‘ $D^{-1}A$ best’’ indicates spectral clustering on the best eigenvector of $D^{-1}A$. Here, $n = 5000$, $c_{\text{out}} = 1$, $c_{\text{in}} = 2 \rightarrow 16$. Average over 10 samples. ‘‘ $D^{-1}A$ best’’ uses the eigenvector giving largest overlap among the first 100.

Remark 3 (Second estimation of ζ). *An alternative approach to estimate ζ consists in evaluating the ratio γ_1/γ_2 between the two dominant (and real) eigenvalues of B . From (3), these can be estimated by a line search over $r \in (\sqrt{\rho(B)}, \infty)$ on changing signs of $\theta_1(r)$ and $\theta_2(r)$ (defined in the previous section) that would correspond to $r = \gamma_1$ and $r = \gamma_2$, respectively.*

Figure 3 displays a superposition of the spectra of three large matrices B ($n = 3000$ nodes) associated with various values for c_{in} and c_{out} but maintaining $c = \frac{1}{2}(c_{\text{in}} + c_{\text{out}})$ constant. The main bulk eigenvalues are kept in blue, while the eigenvalues of interest are stressed in three different colors. Consistently with the claims of (Gulikers et al., 2016), the dominant eigenvalue is approximately constant in the three scenarios and the second largest well approximates $\Phi(c_{\text{in}} - c_{\text{out}})/2$ (marked in dotted lines).

4.2.2. RELATION TO EIGENVALUES IN THE BULK

More interestingly, Figure 3 shows that the rightmost real eigenvalue of B inside the main bulk is a close approximation for ζ (exact values of ζ in dashed lines), a point we believe has never been raised so far. We thus observe that the non-backtracking matrix B has only four real eigenvalues inside its main bulk: $-1, 0, 1$ and ζ (in a two-class scenario). From the relation (3), this behavior is consistent with the observation made in Section 4.1 that $\theta_2(\zeta) = \det[H_\zeta] = 0$. As $c_{\text{in}} - c_{\text{out}}$ decreases, both rightmost eigenvalue inside the bulk of B and leftmost outside together converge to the edge, as shown by arrows in Figure 3.

The connection between B and H_r and the above remarks provide us with two estimation methods (Remarks 2 and 3) for ζ without the need to compute the eigenvalues of B , that we will exploit in our numerical experiments.

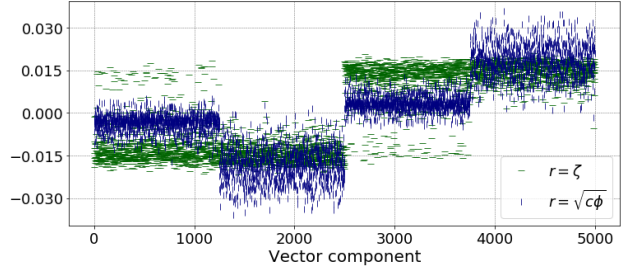


Figure 5. Informative eigenvectors of $D - rA$ for $r = \zeta$ (green) and for $r = \sqrt{c\phi}$ (as proposed in (Saade et al., 2014)) (blue). Here we have $n = 5000$, $c_{\text{in}} = 12$, $c_{\text{out}} = 1$, and $q_i \in \{q_{\text{min}}, q_{\text{max}}\}$ with $q_{\text{max}} = 8q_{\text{min}}$.

4.3. Relation to the Random Walk Operator

We now raise a surprising consequence of the present study in relation with the random walk operator $D^{-1}A$. Similar to A , $D - A$, $D^{-\frac{1}{2}}AD^{-\frac{1}{2}}$, the matrix $D^{-1}A$ (which, in passing, shares the same eigenvalues as those of $D^{-\frac{1}{2}}AD^{-\frac{1}{2}}$ and, up to normalization, the same eigenvectors) is supposed *inappropriate* as a spectral community detection matrix for sparse graphs. We subsequently show that this is in fact an overstatement and that a so far overlooked phenomenon is occurring: as the graph under study gets sparser, $D^{-1}A$ still possesses one or possibly more informative eigenvectors, however no longer corresponding to a dominant isolated eigenvalue.

To understand this statement, similar to our derivation for $D - rA$, we first study how $D^{-1}A$ acts on average on the class vector σ . Precisely,

$$\mathbb{E}[(D^{-1}A\sigma)_i | A] = \mathbb{E}\left[\frac{|\partial_i^{(s)}| - |\partial_i^{(o)}|}{d_i}\right] = \frac{1}{\zeta}\sigma_i$$

and thus, for large d_i , σ is a close eigenvector to $D^{-1}A$. However, while for small ζ (simple problems), the eigenvector of interest is likely associated to a dominant eigenvalue of $D^{-1}A$ (close to $1/\zeta$), as ζ increases in more challenging scenarios, the eigenvector of interest is associated with a small eigenvalue (of order $1/\zeta$) of $D^{-1}A$. Repeating the analysis of Section 3 to $D^{-1}A$ results in similar conclusions, with the key difference that, for hard classification tasks, it is difficult to identify the informative eigenvalue-eigenvector pair, which is problematic in practice. This effect is all the more exacerbated that the graph is heterogeneous and sparse as the bulk of eigenvalues tends to further spread and thus

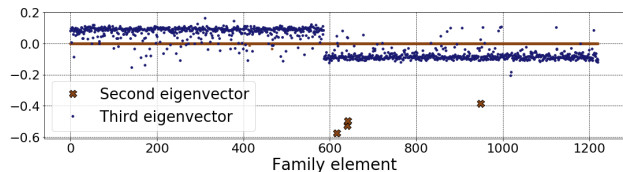


Figure 6. Second and third dominant eigenvectors of $D^{-1}A$ for the Polblogs graph.

easily “absorbs” the eigenvalue of interest.

5. Experimental Validation

5.1. Synthetic Networks

Figure 4 provides an experimental validation for our proposed algorithm, comparing the obtained overlap to state-of-the-art spectral methods: based on $D - \sqrt{\rho(B)}A$ (equivalent to $H_{\sqrt{\rho(B)}}$), $D^{-1}A$, $D^{-1}A$ for the eigenvector reaching maximum overlap (based on oracle choice), and A .

The “Constant” q_i case turns the DC-SBM model into a conventional SBM. The left display of Figure 4 therefore recovers the results of (Saade et al., 2014), evidencing a strong advantage for $D - \sqrt{\rho(B)}A$ (Bethe Hessian) versus all standard Laplacian methods. Interestingly, the overlap achieved by $D - \zeta A$ is indistinguishable to (if not slightly better than) the Bethe Hessian performance.

But the actual improvement provided by $D - \zeta A$ arises for the “Step” distribution case for q_i (right display in Figure 4). Great care is needed to fully grasp this graph. One must first understand that spectral clustering is systematically performed based on two-class k-means clustering of the selected eigenvector. As per Figure 5, the eigenvector of the Bethe Hessian suffers from a spreading (even a full splitting) of the classes induced by the q_i ’s heterogeneity: this severely impedes the k-means performance, especially when the sub-parts of the eigenvector isolate, *i.e.*, for easy tasks. This explains the poor performances of the Bethe Hessian for easy tasks (large α) but also suggests that, while $H_{\sqrt{\rho(B)}}$ visually appears no worse than $D - \zeta A$ for hard tasks (small α), a four-class k-means would likely overtake a two-class k-means thereby overestimating the genuine number of classes.

Regarding the performance of spectral clustering for the random walk operator $D^{-1}A$, as anticipated in Section 4.3, it appears on both displays of Figure 4 that the best eigenvector choice does not coincide with the conventionally considered second largest eigenvector, at least for small values of α (hence non trivial tasks). It is nonetheless surprising at first to observe rather poor performances with respect to $D - \zeta A$ achieved by the (oracle) optimal eigenvector of $D^{-1}A$. This

Graph	A	$D - A$	$D^{-1}A$	$H_{\sqrt{\rho(B)}}$	$D - \zeta A$
Karate	1.0	0.65	0.94	1.0	1.0
Dolphins	0.65	0.97	0.97	0.87	0.97
Adjnoun	0.54	0.03	0.73	0.68	0.68
Polblogs	0.25	0.03	0.03	0.32	0.90

Table 1. Overlap performance on benchmark graphs. The network ‘Adjnoun’ is disassortative, *i.e.*, $c_{in} < c_{out}$; as such, the informative eigenvector is here associated to the smallest eigenvalue and ζ is negative.

is likely due to the fact that, for non trivial clustering, the eigenvalue associated to the optimal eigenvector is no longer isolated but rather immersed in the (dense) main bulk of eigenvalues of $D^{-1}A$; this results in a natural spreading of the expected informative eigenvector to other eigenvectors associated to close-by eigenvalues (as such, spectral clustering on more than a single eigenvector is likely to largely improve the performances).

5.2. Real Networks

To test the robustness of our proposed algorithm to real-life scenarios, Table 1 provides a comparison of the performances of the aforementioned spectral algorithms for the same benchmark graphs as in (Saade et al., 2014), with ζ estimated as per either Remark 2 or Remark 3 (both systematically led to the same overlaps). The performances achieved by $D^{-\frac{1}{2}}AD^{-\frac{1}{2}}$ coincide with those obtained by $D^{-1}A$ and are therefore not presented. As opposed to (Saade et al., 2014) and consistently with the article, we systematically performed a two-class k-means clustering of the chosen eigenvectors rather than a sign-based clustering (which would be inappropriate for classes of uneven sizes and extensions to more than two classes). This explains the differing overlap values with respect to (Saade et al., 2014), especially in the case of Polblogs where the dominant eigenvector for the Bethe Hessian (and interestingly also for the matrix A) has a quite singular form and happens to be best clustered on a sign-based approach: this problem does not occur with $D - \zeta A$.

The results of Table 1 suggest a strong competitive advantage for $D - \zeta A$ on real graphs and thus a resilience of our proposed method to possible model mismatches.

To further confirm the importance of a smart selection of the informative eigenvector of $D^{-1}A$, Figure 6 depicts both its second and third eigenvectors for the Polblogs network. The figure confirms the extremely weak performance achieved by conventional spectral clustering on (the second eigenvector of) $D^{-1}A$ observed in Table 1, while spectral clustering on another eigenvector (here the third) would have resulted in competing performances.

6. Conclusion

The article claims and strongly supports through extensive simulations the competitive advantage brought by spectral clustering on the second smallest eigenvector of $D - \zeta A$ for $\zeta = (c_{\text{in}} + c_{\text{out}})/(c_{\text{in}} - c_{\text{out}})$ for heterogeneous sparse graphs. Through mostly heuristic derivations, we provided a closed-form formulation for the achieved overlap, thereby allowing for an explicit understanding of the impact of heterogeneity on sparse graph clustering. Our main line of argument is however so far mostly heuristic or based on simulated observations, as rigorous mathematical tools are lacking to fully address the problem.

Such mathematical advances are clearly needed to fully grasp community detection on sparse realistic graphs and are a natural next step in this line of investigation. Alternatively, the aforementioned mapping to a statistical physics Ising problem, thereby leading to understanding which “temperature” ensures best clustering properties, is another direction of exploration that may bring further insights. Enriching this toolbox is a mandatory preliminary to address the more general setting of uneven class sizes and the generalization to multiple class clustering.

Acknowledgements

This work is supported by the ANR Project RMT4GRAPH (ANR-14-CE28-0006) and by the IDEX GSTATS Chair at University Grenoble Alpes.

References

- Banks, J., Moore, C., Newman, M., and Zhang, P. Community detection with the z-laplacian. 2014.
- Bordenave, C., Lelarge, M., and Massoulié, L. Non-backtracking spectrum of random graphs: community detection and non-regular ramanujan graphs. In *Foundations of Computer Science (FOCS), 2015 IEEE 56th Annual Symposium on*, pp. 1347–1357. IEEE, 2015.
- Decelle, A., Krzakala, F., Moore, C., and Zdeborová, L. Asymptotic analysis of the stochastic block model for modular networks and its algorithmic applications. *Physical Review E*, 84(6):066106, 2011.
- Fortunato, S. and Hric, D. Community detection in networks: A user guide. *Physics Reports*, 659:1 – 44, 2016.
- Grindrod, P., Higham, D. J., and Noferini, V. The deformed graph laplacian and its applications to network centrality analysis. *SIAM Journal on Matrix Analysis and Applications*, 39(1):310–341, 2018.
- Gulikers, L., Lelarge, M., and Massoulié, L. An impossibility result for reconstruction in a degree-corrected planted-partition model. *arXiv preprint arXiv:1511.00546*, 2015.
- Gulikers, L., Lelarge, M., and Massoulié, L. Non-backtracking spectrum of degree-corrected stochastic block models. *arXiv preprint arXiv:1609.02487*, 2016.
- Gulikers, L., Lelarge, M., and Massoulié, L. A spectral method for community detection in moderately sparse degree-corrected stochastic block models. *Advances in Applied Probability*, 49(3):686–721, 2017.
- Krzakala, F., Moore, C., Mossel, E., Neeman, J., Sly, A., Zdeborová, L., and Zhang, P. Spectral redemption in clustering sparse networks. *Proceedings of the National Academy of Sciences*, 110(52):20935–20940, 2013.
- Lei, J. and Rinaldo, A. Consistency of spectral clustering in stochastic block models. *The Annals of Statistics*, 43(1): 215–237, 2015.
- Massoulié, L. Community detection thresholds and the weak ramanujan property. In *Proceedings of the forty-sixth annual ACM symposium on Theory of computing*, pp. 694–703. ACM, 2014.
- Morbidi, F. The deformed consensus protocol. *Automatica*, 49(10):3049–3055, October 2013. ISSN 00051098.
- Mossel, E., Neeman, J., and Sly, A. Reconstruction and estimation in the planted partition model. *Probability Theory and Related Fields*, 162(3-4):431–461, 2015.
- Nadakuditi, R. R. and Newman, M. E. Graph spectra and the detectability of community structure in networks. *Physical review letters*, 108(18):188701, 2012.
- Rohe, K., Chatterjee, S., Yu, B., et al. Spectral clustering and the high-dimensional stochastic blockmodel. *The Annals of Statistics*, 39(4):1878–1915, 2011.
- Saade, A., Krzakala, F., and Zdeborová, L. Spectral clustering of graphs with the bethe hessian. In *Advances in Neural Information Processing Systems*, pp. 406–414, 2014.
- Terras, A. *Zeta functions of graphs: a stroll through the garden*, volume 128. Cambridge University Press, 2010.
- Tiomoko Ali, H. and Couillet, R. Random matrix improved community detection in heterogeneous networks. In *Signals, Systems and Computers, 2016 50th Asilomar Conference on*, pp. 1385–1389. IEEE, 2016.
- Von Luxburg, U. A tutorial on spectral clustering. *Statistics and computing*, 17(4):395–416, 2007.
- Yedidia, J. S., Freeman, W. T., and Weiss, Y. Constructing free-energy approximations and generalized belief propagation algorithms. *IEEE Transactions on information theory*, 51(7):2282–2312, 2005.